
Technical Note

On load interaction in the non linear buckling analysis of cylindrical shells

LUIS A. GODOY

Departamento de Estructuras, Universidad Nacional de Córdoba, Casilla de Correo 916, 5000 Córdoba, Argentina

SERGIO R. IDELSOHN

INTEC, Universidad Nacional del Litoral, Guemes 3450, Santa Fe 3000, Argentina

EVER BARBERO

Mechanical and Aerospace Engineering, West Virginia University, Morgantown, W.V., U.S.A.

The elastic stability of shells or shell-like structures under two independent load parameters is considered. One of the loads is associated to a limit point form of buckling, whereas the second is a bifurcation. A simple one degree of freedom mechanical system is first investigated, for which an analytical solution is possible. Next, a cylindrical shell under the combined action of axial load and localised lateral pressure is studied via a non linear, two-dimensional, finite element discretization. It is shown that both problems display the same general behaviour, with a stability boundary in the load space which is convex towards the region of stability. The results show the need of performing a full non-linear analysis to evaluate the stability boundary for the class of interaction problems considered.

Key Words

INTRODUCTION

Load interactions arise in the buckling of structures when two or more loads are increased by independent load parameters. For such problems, it is of great importance to evaluate under what combination of load parameters the system will become unstable. A general

theoretical framework on the buckling under combined loading was presented by Huseyin in 1970^{1,2} using an asymptotic formulation in terms of generalised coordinates. In a multidimensional load space, the set of points associated to an initial loss of stability, is called the stability boundary. But not only the values of critical load parameters are important: also the curvature of the stability boundary is of great interesting design. The early studies of Papkovich³ were restricted to bifurcation buckling, and showed that the stability boundary cannot have convexity towards the region of stability in the load space. The practical implications of such statement are that if a any two points of the stability boundary are known (such as the critical points under independent loads), a linear interpolation yields a lower bound to the buckling problem under combined loads. Cylindrical shells under axial load and uniform lateral pressure are an example of such behaviour^{4,5}.

But for structural systems in which the buckling behaviour is not completely defined by bifurcation, the conclusions of Papkovich are no longer valid. For a one degree of freedom and two load parameters, Hueyin² showed that in systems governed by a non-linear behaviour, the stability boundary should have convexity towards the region of stability. Thus, in non linear buckling problems, for which at least one of the loads acting independently is associate to a limit point, a linear stability boundary may constitute an unsafe estimate of buckling load.

In the present work, attention is focused on the non-linear behaviour of elastic cylindrical shells, under two

independent loading parameters, one of which is associated to a limit point form of buckling. First, a simple one degree of freedom system with the above characteristics is analysed in order to consider the main features of the behaviour from the mechanics point of view. Next, the studies are extended to consider a cylindrical shell under axial load and local lateral pressure, which displays a very similar behaviour to the introductory mechanical model. The communication attempts to highlight the type of Finite Element analysis that would be necessary to compute critical loads and stability boundary in this case.

BUCKLING OF A SIMPLE MECHANICAL MODEL WITH TWO LOAD PARAMETERS

In order to illustrate the basic mechanics of the interaction problem, the simple conservative one degree-of-freedom system shown in Fig. 1 is investigated in this section under the combined action of two independent loads. A distinctive feature of the model is that each load, acting independently on the system, is associated to an unstable postbuckling behaviour: the axial load P_1 leads to bifurcation buckling; whereas P_2 is associated to a non linear behaviour with a limit point. It will be seen in the next section that a similar behaviour is displayed by the more complex finite element model of a cylindrical shell.

The total potential energy of the system may be written in the form

$$V = K\Delta^2 - P_2\Delta_2 - 2P_1\Delta_1$$

With reference to Fig. 1, it may be shown that V results in terms of a single displacement parameter $Q = \Delta_2/L$ as

$$V(Q, P_1, P_2) = \frac{1}{4}KL^2\left(Q^2 - \frac{3\sqrt{3}}{4}Q^3\right) - P_1LQ^2 - P_2LQ \quad (2)$$

where terms containing powers of Q higher than 3 have been neglected in the approximation.

Equilibrium of the system is obtained from the condition of stationary potential energy, $\partial V/\partial Q = 0$, while the

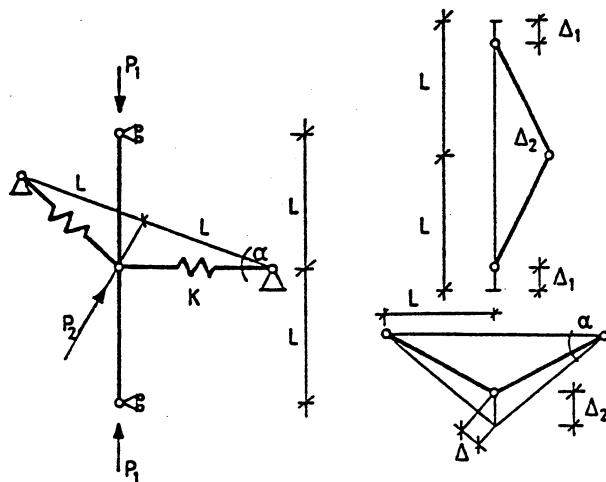


Fig. 1. Geometry, loading and deflections for the one degree of freedom model considered

stability coefficient reduces in this case to $\partial^2 V/\partial Q^2|_E$ evaluated on the equilibrium path E . Critical equilibrium is associated to the condition $\partial^2 V/\partial Q^2|_E = 0$ (see Refs. 6 and 7).

For both loads acting on the system, equilibrium is given by

$$P_1 = \frac{1}{4}KL\left(1 - \frac{9\sqrt{3}}{8}Q\right) - \frac{1}{2}P_2Q^{-1} \quad (3)$$

Notice that for $P_1 = 0$, Equation (3) reduces to

$$P_2 = \frac{1}{2}KL\left(Q - \frac{9\sqrt{3}}{8}Q^2\right) \quad (4)$$

which is a non-linear unstiffening behaviour, and exhibits a limit point at

$$P_2^c = \frac{1}{9\sqrt{3}}KL \quad (5)$$

For $P_2 = 0$, on the other hand, there is a trivial fundamental path $Q = 0$, and a secondary asymmetric path given by

$$P_1 = \frac{1}{4}KL\left(1 - \frac{9\sqrt{3}}{8}Q\right) \quad (6)$$

with a bifurcation load at

$$P_1^c = \frac{1}{4}KL \quad (7)$$

Under both load parameters, a critical point is reached at the following condition:

$$\frac{P_2^c}{KL} = \frac{1}{9\sqrt{3}}\left(1 - 4\frac{P_1^c}{KL}\right)^2 \quad (8)$$

Figure 2 shows the interaction diagram obtained from the load combination at buckling. It may be seen that for this non-linear problem, the stability boundary is convex towards the region of stability. This result is opposed to what would be expected from the theorems of convexity of the fundamental characteristic surface in Ref. 3. Notice that a linearised stability boundary, plotted in Fig. 2, would predict unsafe buckling loads, with an error which increases as buckling is dominated by the transverse load P_2 (associated to a limit-point form of buckling).

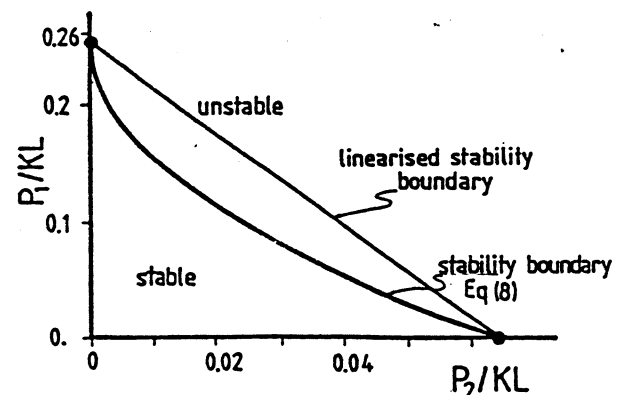


Fig. 2. Stability boundary for the model of Fig. 1

BUCKLING OF CYLINDRICAL SHELLS UNDER COMBINED AXIAL LOAD AND LOCAL LATERAL PRESSURE

In most previous studies on the buckling behaviour of cylindrical shells under combined axial load and lateral pressure, the latter is assumed as uniformly distributed in the circumferential direction. In fact, only in a few cases has the influence of local pressures been considered in a buckling analysis^{8,9}. But in many engineering applications of cylindrical shells, it may be necessary to evaluate stability under axial load and local lateral pressure. This occurs, for example, in the design of shells under wind and gravity load; or in the design of the legs in semi-submersible and tensioned leg off-shore platforms, which are subject to permanent uniform axial load as well as to more localised lateral pressure exerted by waves¹⁰.

Fig 3 shows the geometry and loading of the shell considered. The lateral pressure has been obtained from a study on the slamming of a breaking wave on a cylindrical shell, as modelled in Ref. 11. In the present work it has not been attempted to solve the non-linear dynamic problem, but a static non-linear analysis is carried out at the initial time of wave impact, in which

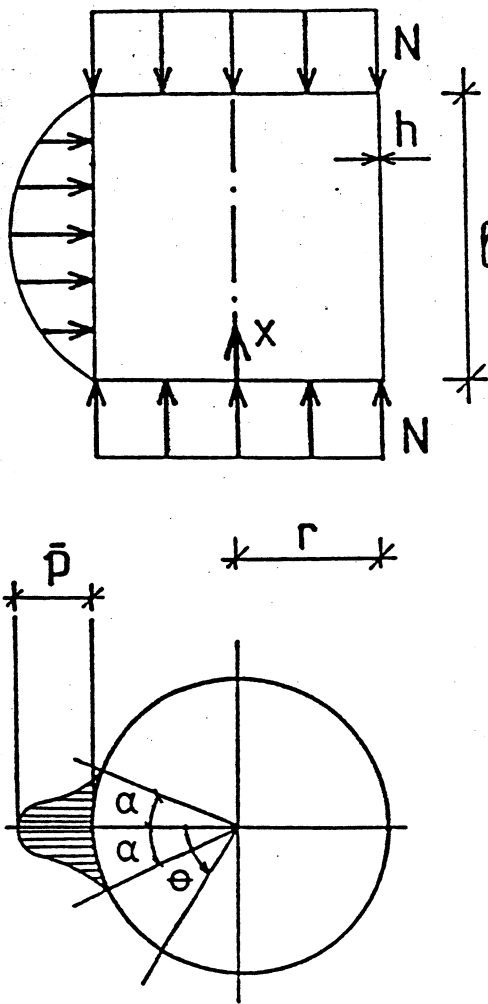


Fig. 3. Dimensions and loading considered for the cylindrical shell. $r = 5000 \text{ mm}$; $h = 25 \text{ mm}$; $l = 10000 \text{ mm}$; $E = 2.05 \times 10^5 \text{ N/mm}^2$; $\nu = 0.3$; $\alpha = \pi/20$

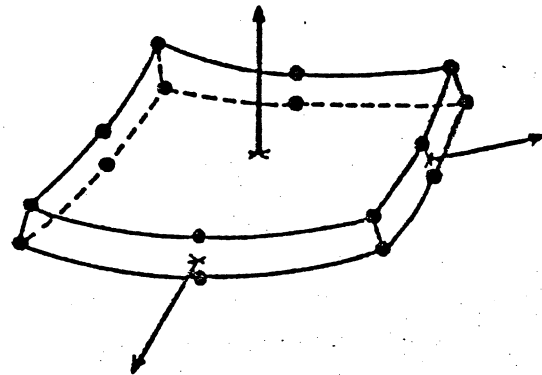


Fig. 4. Sixteen node finite element used in the computations

case the associated lateral pressure is maximum. Following Ref. 11, the pressure distribution is given by

$$p(x, \theta) = \bar{p} \sin\left(\frac{\pi x}{l}\right) \cos^2\left(\frac{\pi \theta}{2\alpha}\right) \quad (9a)$$

$$\text{for } 0 < \theta < \alpha;$$

$$\text{and } p = 0 \quad (9b)$$

$$\text{for } \theta > \alpha$$

where the pressure extends over a central angle 2α , indicated in Fig. 3, with a maximum pressure \bar{p} .

Finite element model

In order to investigate the elastic non-linear behaviour of a cylindrical shell under axial load and local lateral pressure, as defined in the previous section, a two-dimensional shell finite element has been used. The shell is modelled using the 16-node element of Fig 4, which is a degenerated solid element with reduced integration and 48 degrees of freedom. Only geometric non-linearity has been considered, and the constitutive material is assumed to be linearly elastic. The element is based on a Total Lagrangean formulation, and is fully described in Ref. 12. The non-linear equations have been solved using a continuation method¹³.

The finite element discretization extends over a quarter of the shell, with conditions of symmetry being applied at $x = l/2$, $\theta = 0$ and $\theta = \pi$. The boundary conditions at the ends of the shell were assumed as simply supported, with vertical displacements allowed (usually termed SS3 in the literature). The mesh consists of 4 elements in the longitudinal direction and 24 elements in the circumferential direction, so that buckling modes with 6 circumferential waves and a half longitudinal wave could be represented. To check the accuracy of the results, comparisons have been made with an analytical linear dynamic response, and the results were in complete agreement.

Numerical results

A particular steel shell is studied in this section to illustrate some of the main features of the buckling behaviour under combined axial load and local lateral pressure. The shell dimensions were taken from Ref. 11 as

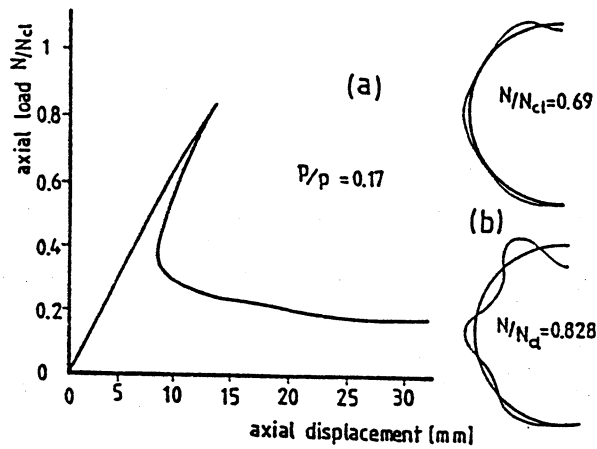


Fig. 5. Buckling under axial dominated load. (a) Load-displacement path at $x = 0, \theta = 0$; (b) Out of plane displacement at several load levels

$r = 5,000$ mm; $h = 25$ mm; and $l = 10,000$ mm; leading to slenderness ratios $r/h = 200$; $l/r = 2$ and Bartdorf parameter $Z = 76$.

First, the buckling behaviour under axial dominated load will be investigated, in which case the shell is loaded by a local pressure of constant maximum value $\bar{p} = 0.0284 N/mm^2$ and the axial load is increased. Fig 5a shows the load displacement path obtained from the finite element non-linear analysis, and in which the axial load N has been normalised with respect to the classical critical value

$$N_{cl} = 0.605E \frac{h^2}{r} \quad (10)$$

while the lateral maximum pressure has been normalised with respect to that obtained from the equation of Yamaki

$$P_{cl} = \frac{0.855E}{(r/h)^{2.5} l/r (1 - \nu^2)^{0.75}} \quad (11)$$

A maximum load is achieved at $N/N_{cl} = 0.828$; as expected, the load decreases sharply in the post-buckling path under controlled displacements. A minimum value is registered at $N/N_{cl} = 0.118$. The buckling mode is shown in Fig. 5b at three different load levels. Even for this relatively small lateral pressure, the buckling mode is severely affected by the pressure, with the largest displacements occurring in the area of maximum lateral pressure.

Second, the shell behaviour under a constant axial load $N/N_{cl} = 0.15$ and increasing local pressure has been studied. The load-deflection path is shown in Fig 6a, in which the out-of-plane displacement is measured at $x = l/2$ and $\theta = 0$. The response is now highly non-linear, with a maximum pressure $p/p_{cl} = 1.5$ calculated for a displacement of 3.7 times the thickness of the shell; and a minimum pressure $p/p_{cl} = 1.10$ after the limit point. The mode of deformation of the shell is represented in Fig. 6b.

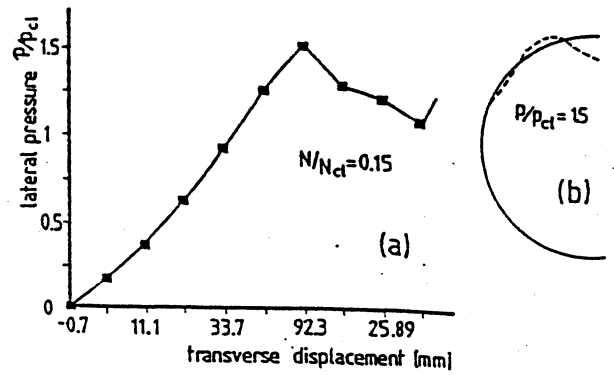


Fig. 6. Buckling under local lateral dominated pressure. (a) Load-displacement path at $x = l/2, \theta = 0$ (b) Out of plane displacement

Next, the results for several load combinations have been plotted in Fig. 7 to show the interaction between axial load and local pressure. The solid line indicates the limit load values and it may be seen that the shell can sustain on a small area a lateral action of higher pressure intensity than the uniform pressure that buckles the shell.

As a reference value, bifurcation buckling loads under a non-axisymmetric fundamental state have been computed using a finite element code described in Ref. 14. The results indicate that as the lateral pressure increases, the difference between limit and bifurcation points become larger. The reason for this is that the bifurcation load is calculated from a linear fundamental path, while the results of Fig. 6a show that the load-displacement path before buckling involves large displacements. Thus, a bifurcation analysis leads to meaningless results in the present case.

Notice that the behaviour of the cylindrical shell under combined loading is similar to the simple mechanical model discussed above, with the loads N, p being associated to P_1, P_2 .

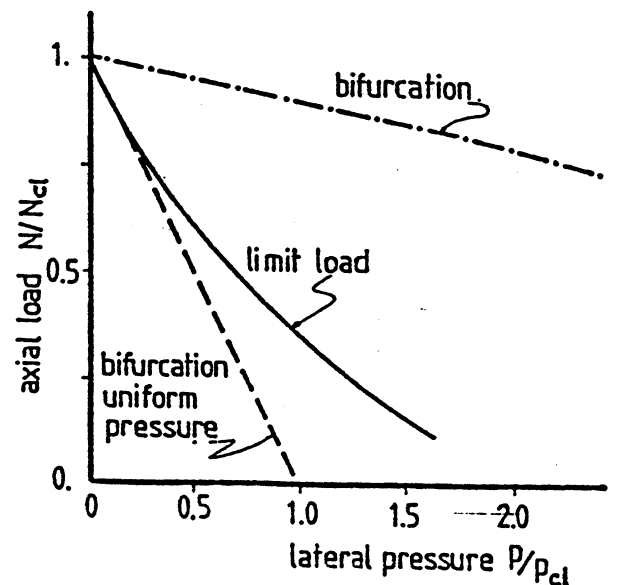


Fig. 7. Stability boundary for the cylindrical shell under axial load and local lateral pressure

BUCKLING OF CYLINDRICAL SHELLS UNDER COMBINED AXIAL LOAD AND LOCAL LATERAL PRESSURE

In most previous studies on the buckling behaviour of cylindrical shells under combined axial load and lateral pressure, the latter is assumed as uniformly distributed in the circumferential direction. In fact, only in a few cases has the influence of local pressures been considered in a buckling analysis^{8,9}. But in many engineering applications of cylindrical shells, it may be necessary to evaluate stability under axial load and local lateral pressure. This occurs, for example, in the design of shells under wind and gravity load; or in the design of the legs in semi-submersible and tensioned leg off-shore platforms, which are subject to permanent uniform axial load as well as to more localised lateral pressure exerted by waves¹⁰.

Fig 3 shows the geometry and loading of the shell considered. The lateral pressure has been obtained from a study on the slamming of a breaking wave on a cylindrical shell, as modelled in Ref. 11. In the present work it has not been attempted to solve the non-linear dynamic problem, but a static non-linear analysis is carried out at the initial time of wave impact, in which

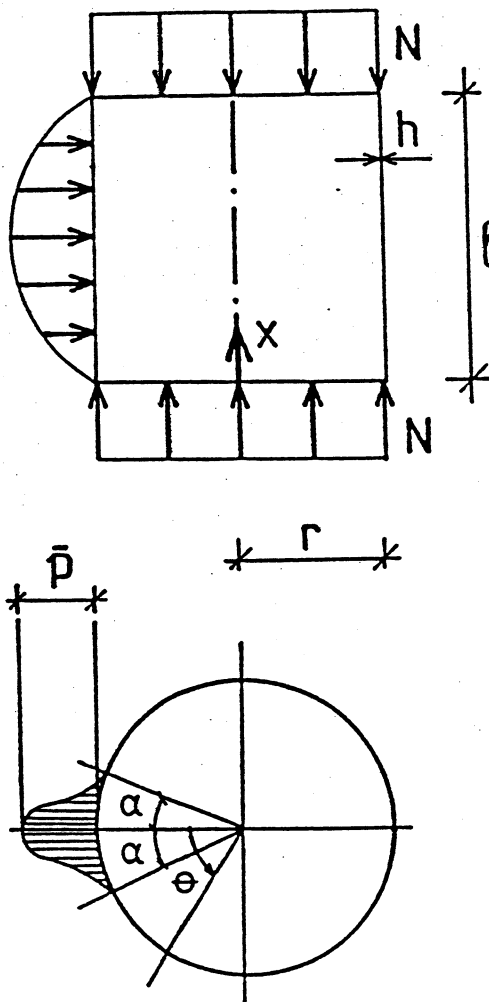


Fig. 3. Dimensions and loading considered for the cylindrical shell. $r = 5000 \text{ mm}$; $h = 25 \text{ mm}$; $l = 10000 \text{ mm}$; $E = 2.05 \times 10^5 \text{ N/mm}^2$; $\nu = 0.3$; $\alpha = \pi/20$

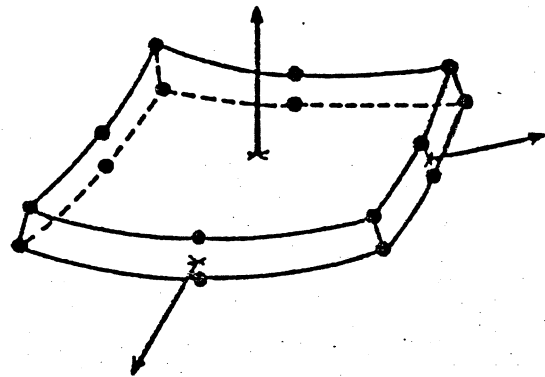


Fig. 4. Sixteen node finite element used in the computations

case the associated lateral pressure is maximum. Following Ref. 11, the pressure distribution is given by

$$p(x, \theta) = \bar{p} \sin\left(\frac{\pi x}{l}\right) \cos^2\left(\frac{\pi \theta}{2\alpha}\right) \quad (9a)$$

$$\text{for } 0 < \theta < \alpha;$$

$$\text{and } p = 0 \quad (9b)$$

$$\text{for } \theta > \alpha$$

where the pressure extends over a central angle 2α , indicated in Fig. 3, with a maximum pressure \bar{p} .

Finite element model

In order to investigate the elastic non-linear behaviour of a cylindrical shell under axial load and local lateral pressure, as defined in the previous section, a two-dimensional shell finite element has been used. The shell is modelled using the 16-node element of Fig 4, which is a degenerated solid element with reduced integration and 48 degrees of freedom. Only geometric non-linearity has been considered, and the constitutive material is assumed to be linearly elastic. The element is based on a Total Lagrangean formulation, and is fully described in Ref. 12. The non-linear equations have been solved using a continuation method¹³.

The finite element discretization extends over a quarter of the shell, with conditions of symmetry being applied at $x = 1/2$, $\theta = 0$ and $\theta = \pi$. The boundary conditions at the ends of the shell were assumed as simply supported, with vertical displacements allowed (usually termed SS3 in the literature). The mesh consists of 4 elements in the longitudinal direction and 24 elements in the circumferential direction, so that buckling modes with 6 circumferential waves and a half longitudinal wave could be represented. To check the accuracy of the results, comparisons have been made with an analytical linear dynamic response, and the results were in complete agreement.

Numerical results

A particular steel shell is studied in this section to illustrate some of the main features of the buckling behaviour under combined axial load and local lateral pressure. The shell dimensions were taken from Ref. 11 as